RKCL4651

INFLUENCE OF OH/METAL RATIO ON THE STABILITY OF AlFe-PILC CATALYST FOR WET PEROXIDE OXIDATION OF PHENOL

Ernő E. Kiss[*], Tatjana J. Vulić, Goran C. Bošković,
Andreas F.K. Reitzmann[a] and Károly Lázár[b]

University of Novi Sad, Faculty of Technology, Bul.Cara Lazara 1,
21000 Novi Sad, Serbia and Montenegro
[a]Institute for Chemical Process Engineering, University of Karlsruhe (TH), Germany
[b]Institute of Isotopes of the Hungarian Academy of Sciences, Department of Catalysis and Tracer
Studies, P. O. Box 77 Budapest, H-1525 Hungary

Abstract

AlFe-pillared clay catalyst with OH/metal = 4; 5 mmol metal/g clay and Al : Fe = 5 : 5 swells intensively in phenol-water solution and has no measurable catalytic activity in phenol removal from water solutions, in contrast to the similar catalyst with OH/metal = 2. The different behavior of two samples can be explained first of all by differences in iron ion distribution in the catalysts as a consequence of applied pillaring solutions prepared at different OH/metal ratios. In the sample with OH/metal = 2 iron ions are uniformly distributed on the AlFe-pillars, while in the sample with OH/metal = 4 iron ions appear not only on the pillars but also as a bulk $FeO \cdot Fe_2O_3$-form. The results obtained by FTIR, SEM, TPR and Mössbauer spectroscopy reveal the differences in acid-base properties, morphology and iron ion distribution in the samples.

Keywords: AlFe-pillared montmorillonite, OH/metal ratio, phenol decomposition

INTRODUCTION

AlFe-pillared clays (AlFe-PILC) are efficient solid catalysts for the oxidation of organic compounds with hydrogen peroxide in water solutions [1-3]. Their properties such as acidity, surface area, pore size distribution and

*Corresponding author. E-mail: ekiss@tehnol.ns.ac.yu

hydrothermal stability depend on the method of synthesis, pH, temperature, OH/metal ratio, *etc.*, as well as on the host clay. In our previous works [2, 3] we have referred about catalytic wet peroxide oxidation of phenol over AlFe-PILC (OH/metal = 2) with different iron ion content. In our later experiments we have studied this reaction on AlFe-PILC catalyst synthesized with OH/metal = 4; 5 mmol metal/g clay and Al : Fe = 5 : 5. However, this catalyst swells intensively in phenol-water solution and has no measurable catalytic activity in phenol removal from water solutions, on the contrary to the similar catalyst with OH/metal = 2. We do not exclude catalytic activity of this catalyst in phenol removal from water solution, however, it is difficult to measure it by the applied photo-analytical technique requiring perfectly transparent solutions [4]. We dismissed further investigations with this catalyst in phenol removal reactions from water solutions, because such unstable catalyst can cause serious water pollution with iron ions. However, this catalyst has shown a significant catalytic activity in N_2O reduction with NH_3 [5]. The activity test was carried out in the same reactor as described elsewhere [6]. The aim of this work is to figure out the physico-chemical differences between two samples which may be important for different catalytic behavior of these samples. In later discussion the catalyst successfully applied for N_2O decomposition is marked as Al : Fe = 5 : 5(4) and the catalyst successfully used in our previous works for phenol conversion in water solutions is marked as Al : Fe = 5 : 5(2).

EXPERIMENTAL

The purified parent bentonite clay, Ca-type (Šipovo, Republic Srpska) was used for AlFe-PILC preparation as described in our previous work [3]. The main characteristics of the resulted samples are 5 mmol metal/g clay; Al : Fe = 5 : 5; OH/metal = 4, for sample Al : Fe = 5 : 5(4) and OH/metal = 2, for sample; Al : Fe = 5 : 5(2).

Physico-chemical characterization

XRD analysis, Philips APD 1700 $Cu_{K\alpha}$ in the range $2\theta=3-15$, was applied in structural investigations.

Textural properties were examined by low temperature N_2 adsorption/desorption (LTNA), Micromeritics ASAP 2000. BET adsorption isotherm and *t*-plot were applied in data processing. The pores diameter was determined by pore size distribution curve as dV/dlogD.

The morphology of gold coated samples was studied by scanning electron microscopy (SEM) JEOL JSM-6460LV.

The acid-base properties were studied by FTIR spectrophotometry (Thermo Nicolet Nexus 670) after pyridine adsorption in the range of 1440-1580 cm^{-1}.

For temperature-programmed reductions (TPR), a 10 mL H_2/min + 30 mL Ar/min mixture was passed through a Pyrex glass reactor containing 0.5 g sample. The reactor temperature was ramped at a rate of 10°C/min. The water formed was trapped at − 40°C downstream. A thermal conductivity detector was used to follow and record H_2 consumption.

^{57}Fe Mössbauer spectra were recorded in an *in situ* cell at 77 K and 300 K. A ^{57}Co/Cr source was used in constant acceleration mode. The isomer shifts are relative to metallic α-Fe°. Spectra were computer-fitted and isomer shifts, quadrupole splittings, relative intensities, *etc.* were deduced.

RESULTS AND DISCUSSION

Structural and textural properties

The basal spacing of dried ($d_{(001)}$ = 1.803 nm) and calcined ($d_{(001)}$ = 1.780 nm) samples are determined by the height of the aluminum oxide pillars, and the OH/metal ratio did not influence significantly this value.

The textural properties of samples are given in Table 1. BET surface area and pore volume of prepared PILC samples are higher than the corresponding values of unmodified montmorillonite. BET surface area of Al : Fe = 5 : 5(4) sample is 154.9 m^2/g and that of Al : Fe = 5 : 5(2) sample, 158.7 m^2/g. These surface areas are at the lower range limit for pillar clay materials [7]. The shape of PILC samples adsorption isotherms is somewhere between type I and IV referring to IUPAC classification, indicating microporous/mesoporous type of material [8]. The hysteresis loops, as expected, indicate the presence of slit shaped pores [9].

Table 1

Textural properties of the samples calcined at 300°C, 2h

Sample	S_{BET} m^2/g	P cm^3/g	S_{micro} m^2/g	P_{micro} cm^3/g	d nm	d [4V/S] nm
Montmorillonite	105.5	0.1131	33.0	0.0151	4.0	4.3
AlFe5/5(2)	158.7	0.1599	22.7	0.0094	3.2	4.0
AlFe5/5(4)	154.9	0.1873	18.4	0.0073	2.7	4.8

The samples have very similar structural and textural properties. Therefore, the reason for different catalytic properties has to be looked for in differences in surface acidity and iron ion distribution. .
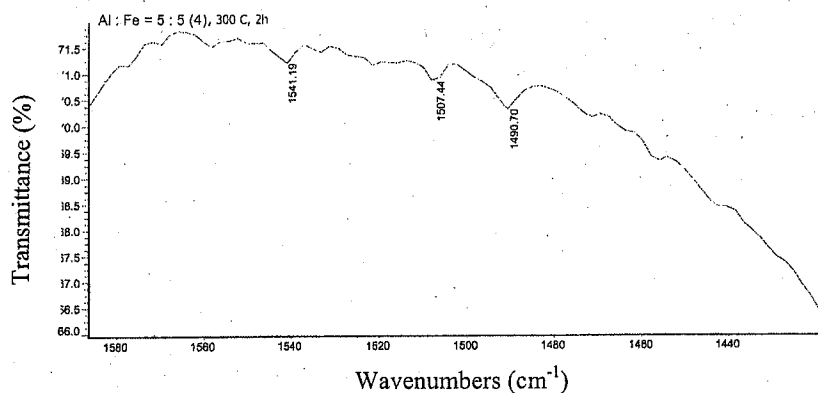

Fig. 1. IR spectra of pyridine adsorbed on Al : Fe = 5 : 5(4) pillared clay
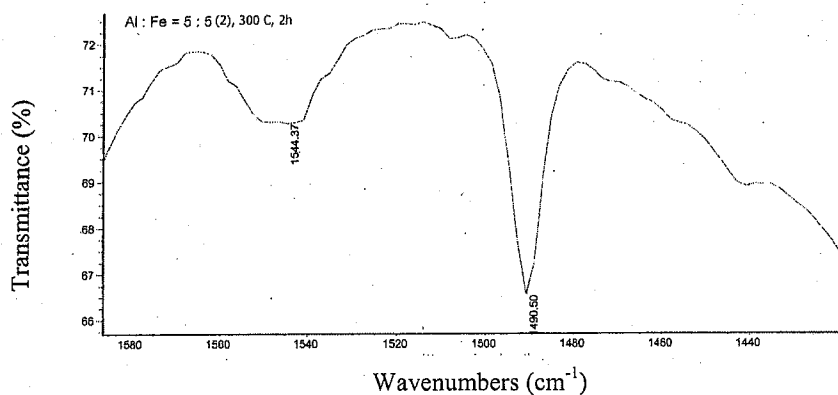

Fig. 2. IR spectra of pyridine adsorbed on Al : Fe = 5 : 5(2) pillared clay

Surface acidity

The amount of Lewis and Brönsted acid sites in Al : Fe = 5 : 5 (4) sample is smaller than in Al : Fe = 5 : 5 (2) sample, Figs 1 and 2. The differences could be explained both by formation of different forms of sodium aluminates

$Al(OH)_4^-/Al(OH)_6^{3-}$ and hydrous iron oxides γ-FeOOH/α-FeOOH as byproducts [10] during the formation of the Keggin ions $[AlO_4Al_{12}(OH)_{24}(H_2O)_{12}]^{7+}$. The pyridine chemisorbed on Brönsted sites is characterized with band at 1545 cm^{-1}, and the pyridine chemisorbed on Lewis sites is characterized with bands at 1452 and 1577 cm^{-1} [11]. The ratio between Lewis and Brönsted acid sites can be estimated from the intensities of the 1490 and 1450 cm^{-1} bands.

TPR measurements

To estimate the degree of iron distribution in pillared clay samples TPR measurements were carried out. The OH/metal ratio has a significant influence on the H_2 consumption of the samples. The starting temperature of hydrogen consumption is similar in both samples i.e. 265/268°C. However, the amount of hydrogen consumption is about 3.5 times smaller in the sample Al : Fe = 5 : 5(2) than in sample Al : Fe = 5 : 5(4). The H_2 consumption curve of sample Al : Fe = 5 : 5(2) is flat in a broad temperature range, 265-500°C, without a clear extreme of the peak temperature. This type of TPR curve let us anticipate that the iron oxide component is homogeneously distributed on the surface of aluminum oxide pillars. The TPR curve of the sample Al : Fe = 5 : 5(4) has a different shape than the TPR curve of the sample Al : Fe = 5 : 5(2). The hydrogen consumption in the sample Al : Fe = 5 : 5(4) proceed faster and reach its maximum at 417°C. The week inversion at 327°C and 380°C suggest the presence of differently coordinated iron oxide species (Figs 3 and 4). After dehydroxylation of unstable γ-FeOOH and α-FeOOH follow the formation of γ-Fe$_2$O$_3$ and FeO. Fe$_2$O$_3$. Both of these iron oxides have a spinel structure, so their reversible transformation proceeds easily, and the final form of iron oxide product will be determined with the oxygen pressure and temperature [10].
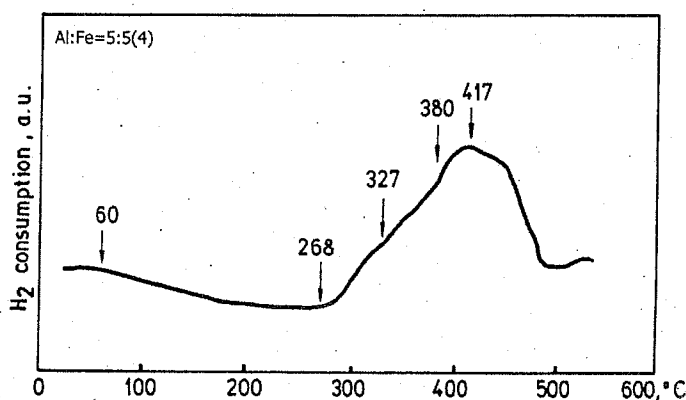

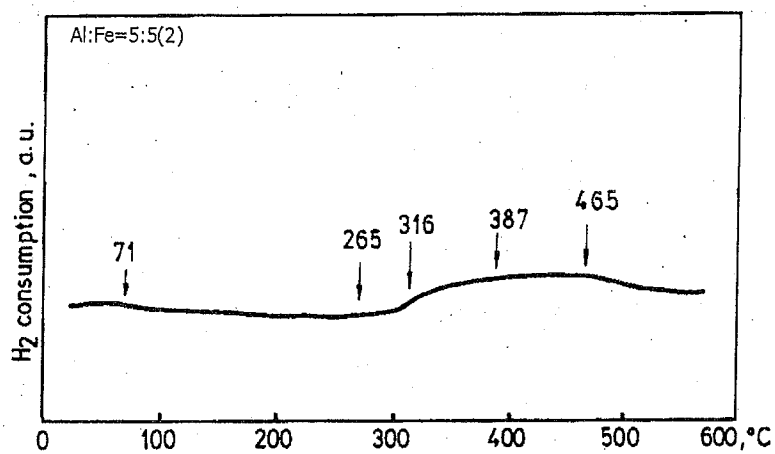Fig. 3. TPR curve of the Al : Fe = 5 : 5(4) pillared clay

Fig. 4. TPR curve of the Al : Fe = 5 : 5(2) pillared clay

Mössbauer measurements

The Mössbauer spectra of the samples are shown in Fig. 5, and the data extracted from the obtained spectra at 300 K and at 77 K are given in Table 2.
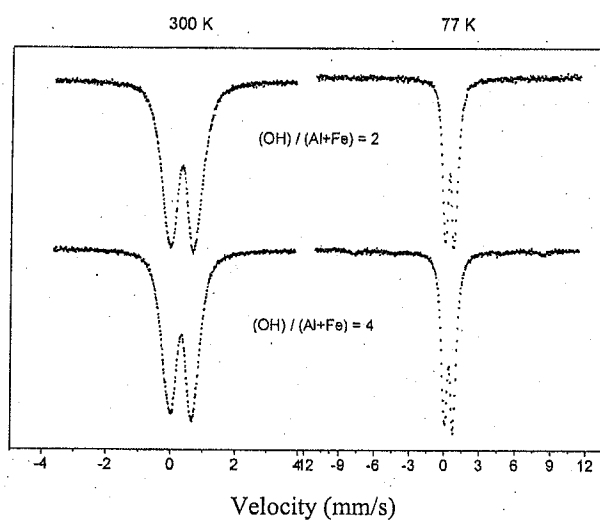

Velocity (mm/s)

Fig. 5. Mössbauer spectra of the Al : Fe = 5 : 5(2) and the Al : Fe = 5 : 5(4) pillared clays

Table 2

Mössbauer date of the Al : Fe = 5 : 5(2) and the Al : Fe = 5 : 5(4) pillared clays

Sample	Temp./K	300	300	300	300	77	77	77	77	77
OH/Me	Comp	IS	QS	HW	RI	IS	QS	MHF	HW	RI
2	$Fe^{3+}(1)$	0.27	0.66	0.33	31	0.25	0.90	-	0.25	8
2	$Fe^{3+}(2)$	0.34	1.18	0.49	36					
2	$Fe^{3+}(3)$	0.43	0.65	0.33	33	0.48	0.79	-	0.56	92
4	$Fe^{3+}(1)$	0.27	0.61	0.32	31	0.24	0.88	-	0.30	7
4	$Fe^{3+}(2)$	0.34	1.08	0.42	33					
4	$Fe^{3+}(3)$	0.41	0.60	0.32	36	0.47	0.74	-	0.58	85
4	$Fe^{3+}_{magn.}$					0.33	-	49.7	1.04	8

In sample Al : Fe = 5 : 5(2) at 77 K (liquid nitrogen) two species of Fe^{3+} ions are present. The smaller part of Fe^{3+} ions (8%) is maybe in octahedral coordination in Keggin ion, since Al^{3+} ion substitution in tetrahedral position with Fe^{3+} ions did not occur [12]. The majority of Fe^{3+} ions (92%) create a homogeneous layer/decoration on the surface of aluminum oxide pillars.

In the sample Al : Fe = 5 : 5(4) beside two mentioned species of Fe^{3+} ions (7%+85%) appears a third one (8%), probably in the form of free clusters which did not take part in aluminum oxide pillars "decoration". These free iron oxide clusters were formed during the fast precipitation of Fe^{3+} ions in the strong basic milieu. The presence of this third type of Fe^{3+} ion species can probably contribute to the fast disintegration of Al : Fe = 5 : 5(4) sample in water solutions. At 300 K, in both samples, the Fe^{3+} ion distribution is similar.

SEM analysis

Catalyst Al : Fe = 5 : 5(2) shows a regular lamellar structure with particles in face-to-face arrangement (Fig. 7). However, sample Al : Fe = 5 : 5(4) shows a less regular structure often with particles in face-to-edge arrangement (Fig. 6). The disturbed particles arrangement in sample Al : Fe = 5 : 5(4) is the consequence of the faster precipitation of iron ions in the more basic environment. The disturbed particles arrangement may be one of the causes of its undesirable behavior in water solutions.

Fig. 6. SEM picture of Al : Fe = 5 : 5(4) pillared clay, magnification 100,000 x

Fig. 7. SEM picture of Al : Fe=5 : 5(2) pillared clay, magnification 100,000 x

CONCLUSION

The Al : Fe = 5 : 5(4) catalyst swells intensively in phenol-water solutions and has no measurable catalytic activity in phenol conversion reaction on the contrary to the Al : Fe = 5 : 5(2) catalyst. Different catalytic behavior of these two samples can be explained by different coordination and distribution of Fe^{3+} ions. In the catalyst sample Al : Fe = 5 : 5(2) the Fe^{3+} ions are practically uniformly distributed on the aluminium oxide pillars, while in the sample Al : Fe = 5 : 5(4) Fe^{3+} ions appear not only on the pillars but also as a bulk $FeO \cdot Fe_2O_3$-form. The results obtained by temperature programmed reduction and Mössbauer spectroscopy also reveal the differences in iron ion distribution.

REFERENCES

1. J. Barrault Jr., C. Bouchoule, J.-M. Tatibuet, M. Abdellaoni, A. Majeste, I. Louloudi, N. Papajannakos, N. H. Ganges: *Stud. Surf. Sci. Catal.,* **130,** 749 (2000).
2. E.E. Kiss, J.G. Ranogajec, R.P. Marinkovic-Neducin, T. Vulic: *React. Kinet. Catal. Lett.,* **80,** 255 (2003).
3. E.E. Kiss, Matilda M. Lazic, Goran C. Boskovic: *RKCL,* **83,** 221 (2004).
4. Ju. Ju.Lur'e: *Analytical Chemistry of Industrial Waste Waters (in Russian),* p. 374-378. Khimija, Moscow 1984.
5. E. Kiss, T. Vulić, G. Bosković, M. Lazić, K. Lázár: *Proc. 4th Int. Conf. of the Chemical Societies of the South-East European Countries, Book of Abstracts, Vol. II,* B-P21, p.181, Belgrade, July 18-21, 2004.
6. T. Vulić, A. Reitzmann, B. Kraushaar-Czarnetzki, *in* Wissenschaftliche Abschlussberichte, 38. Internationales Seminar für Forschung und Lehre in Chemieingenieurwesen, Technischer und Physikalischer Chemie, pp.56-65, Universität Karlsruhe (TH), Germany, July 2003.
7. D.E.W. Vaughan: *US Patent,* 4,666,877, May 19, 1987.
8. S. Wang, H.Y. Zhu, G.Q. (Max) Lu: *J. Coll. Interface Sci.,* **204,** 128 (1998).
9. P. Cañizares, J.L. Valverde, M.R. Sun Kou, C.B. Molina: *Microporous and Mesoporous Materials,* **29,** 267 (1999).
10. I. Filipović, S. Lipanović: Opća i anorganska kemija, II Dio, pp.875-882 and pp.1015-1036, Školska knjiga, Zagreb, 1987.
11. M. Lenarda, R. Ganzerla, L. Storaro, S. Enzo, R. Zanoni: *J. Mol. Catal.,* **92,** 201 (1994).
12. J.B. Nagy, J.-C. Bertrand, I. Pálinkó, I. Kiricsi: *Stud. Surf. Sci. Catal.,* **105C,** 1957 (1997).